Coherent phonon scattering effects on thermal transport in thin semiconductor nanowires

P. G. Murphy and J. E. Moore

Department of Physics, University of California, Berkeley, California 94720, USA
and Materials Sciences Division, Lawrence Berkeley National Laboratory, Berkeley, California 94720, USA

The thermal conductance by phonons of a quasi-one-dimensional solid with isotope or defect scattering is studied using the Landauer formalism for thermal transport. The conductance shows a crossover from localized to Ohmic behavior, just as for electrons; however, the nature of this crossover is modified by delocalization of phonons at low frequency. A scalable numerical transfer-matrix technique is developed and applied to model quasi-one-dimensional systems in order to confirm simple analytic predictions. We argue that existing thermal conductivity data on semiconductor nanowires, showing an unexpected linear temperature dependence, can be understood through a model that combines incoherent surface scattering for short-wavelength phonons with nearly ballistic long-wavelength phonons. It is also found that even when strong phonon localization effects would be observed if defects are distributed throughout the wire, localization effects are much weaker when defects are only at the boundary, as in current experiments.

I. INTRODUCTION

The transport of heat by phonons in quasi-one-dimensional structures is sensitive to quantum confinement effects once the phonon wavelengths that dominate thermal transport are comparable to the structure dimensions. Strong quantum confinement in thermal transport has been demonstrated in the observation[1] of the thermal conductance quantum[2–4] at temperatures $T \lesssim 1$ K and also in recent experiments on semiconductor nanowires[5,6] and nanotubes[7] at higher temperatures (down to ~10 K).

Experiments on the thinnest nanowires are not well explained by current models of independent scattering events at the boundary,[8] even though such models describe thicker wires quite well (see Fig. 1). In particular, data on a 22 nm Si nanowire[5] show thermal conductivity scaling with temperature up to temperatures of order 200 K, well above the temperature where higher transverse modes should be occupied; linear temperature dependence[1] is expected when only the four gapless modes are occupied. This paper studies the effect of coherence between different scattering events in quasi-one-dimensional systems of variable transverse dimension, using a large-scale numerical transfer-matrix approach to check simple analytic models. The differences between bulk and boundary disorder are studied,[9–11] and linear temperature dependence at high temperature is found to depend on having boundary disorder rather than bulk disorder.

The study of quantum effects on electrons in quasi-one-dimensional systems has developed steadily since the observation in 1988 of quantized electrical conductance in ballistic quantum point contacts.[12] The electrical conductance as a function of gate voltage shows plateaus at multiples of $G_e = 2e^2/h$, where h is Planck's constant and e the electron charge, and the factor of 2 results from spin. Hence G_e is a universal conductance quantum for fermions and insensitive to material properties. The corresponding thermal conductance quantum has recently been measured in low-temperature heat transport through small insulating structures:[1] at the lowest energies the only modes accessible

in this system are four phonon modes, and the observed thermal conductance at the lowest temperatures is

$$G = 4g_0 = 4\frac{\pi^2 k_B^2 T}{3h}, \tag{1}$$

where T is temperature and k_B the Boltzmann constant. This thermal conductance quantum is also insensitive to material properties, and is, in addition, independent of the statistics of the particles transporting the heat.[13,14]

This paper studies how scattering and localization by disorder appear in the thermal conductance of long quasi-one-dimensional structures. We restrict ourselves only to low temperatures and coherent processes: phase-breaking processes such as inelastic scattering are neglected. Previous work on coherent scattering in phonon transport has concentrated on the strictly one-dimensional limit;[15] as explained below, there are fundamental aspects of phonon confinement even in the clean case that are not well captured by a purely one-dimensional (1D) chain. We find several important differences between scattering and localization effects in 1D phonon transport and the corresponding effects in electrical transport. As in the electronic problem, transport in quasi-1D systems can be ballistic, diffusive, or localized, but unlike the electronic problem, the lowest four harmonic modes are protected from scattering as $T \rightarrow 0$ by fundamental properties of rigid bodies (in the same way as the three acoustic modes of bulk solids). In order to access very large system sizes, many of our numerical calculations are carried out in two rather than three spatial dimensions; however, two-dimensional systems already include some important features absent in one dimension, e.g., different dispersion relations for the lowest-lying modes ($\omega \sim k$ for torsional and longitudinal, and $\omega \sim k^2$ for transverse). This paper presents two separate approaches to understanding the thermal conductance of these thin nanorods. Firstly, we use a scalar model to study the mean free path of different phonon modes. We find that the gapless mode (which has no transverse wave vector) has a mean free path significantly longer
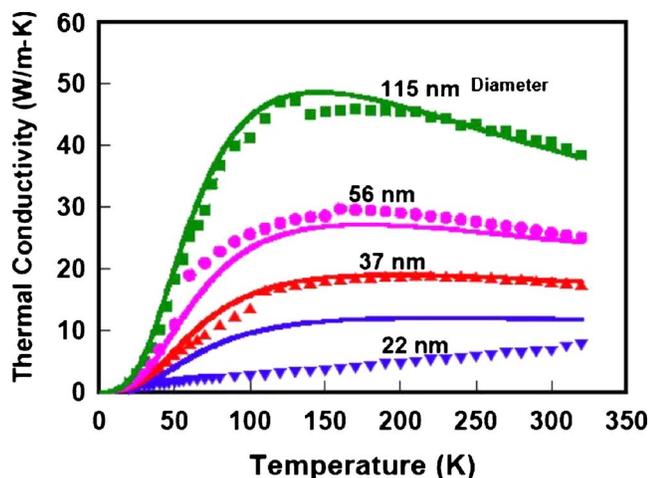
FIG. 1. (Color online) The thermal conductance as a function of temperature for various wire diameters. The fit (solid lines) matches the data to a Boltzmann equation treatment including impurity, surface, and umklapp scattering. Note that the 22 nm wire is anomalous. These data are taken from Ref. 5; the fit (except for d =22 nm) is from Ref. 8; figure courtesy of A. Majumdar.

than the length of the system; when combined with the contribution of the other modes, the resulting thermal conductance for very thin rods (of order 20 nm) is approximately linear.

We also obtain the thermal conductance at low temperature by numerical transfer-matrix calculations on systems of small transverse dimension and an analytic theory that makes standard mesoscopic assumptions about the nature of scattering. Calculations are done using the Landauer formalism valid at low temperatures.[2,16–18] The analytic results for boundary scattering build on the scalar approximation are introduced in Ref. 19. The coherent multiple scattering discussed in this paper is much more important in long nanowires and nanotubes, where the ratio of length to width may be 100:1, than in the suspended membrane devices studied in Ref. 1, where nonuniform width and individual scattering effects have been shown to explain the experimental data.[3,17]

The results obtained here suggest that the experimentally observed dip in G/T at moderate temperatures, discussed in detail for the experimental geometry of Ref. 1 in Ref. 3, will appear generically in one-dimensional systems as a consequence of delocalization of phonons at low energy and 1D-three-dimensional (3D) crossover at high energy. Our theoretical predictions are also compared to experiments on semiconductor nanowires at relatively high temperature as a function of diameter.[5] We find that, while the linear temperature dependence on the smallest nanowire in this experiment is a robust phenomenon, the coefficient does not need to be close to $4g_0$, although it happens to be remarkably close to this value in that experiment.

We use the term "phonon" to describe both long-wavelength bulk modes of the nanowire and conventional short-wavelength phonons as there is no sharp distinction between these two limits. Note that phonon localization by strong local scattering can occur also in dimensions $\mathcal{D} > 1$ (a review is Ref. 20), but considerably more disorder is re-

quired. The following section discusses the basic theory of mesoscopic thermal transport in harmonic quasi-one-dimensional systems: localization is described by the DMPK (named for Dorokhov, Mello, Pereyra, and Kumar)[21–23] model with appropriate modifications. In Sec. III we argue for the relevance of Anderson localization and mode inequivalence for thin nanowires. Section IV contains numerical studies of a two-dimensional (2D) model to understand the key differences between phonon and electron mesoscopics and test the DMPK model, and Sec. V applies this model to three-dimensional nanowires at low temperature.

II. MESOSCOPIC THERMAL TRANSPORT

Our approach is based on the thermal analog of the Landauer formalism for electronic transport. The net thermal current in a wire from a reservoir at temperature $T + \delta T$ to one at temperature T is the difference between that for the phonons traveling to the right minus that for the phonons traveling to the left as follows:

$$J = \sum_i \int \frac{dk}{2\pi} \hbar \omega_i(k) v_i(k) \frac{1}{e^{\hbar \omega_i(k)/k_B(T+\delta T)} - 1} \mathcal{T}_i(\omega_i(k))$$

$$- \sum_i \int \frac{dk}{2\pi} \hbar \omega_i(k) v_i(k) \frac{1}{e^{\hbar \omega_i(k)/k_B T} - 1} \mathcal{T}_i(\omega_i(k)). \quad (2)$$

Here the summation index i runs over all propagating phonon modes and $\mathcal{T}_i(\omega)$ is a transmission probability of phonons in mode i at frequency ω, defined more precisely in terms of the heat flux below. The boundary condition is that a possibly disordered segment of finite length is connected at both ends to infinite reservoirs with no disorder. Note that the distribution in the center of the wire is *not* a thermal distribution, and has no well-defined temperature: the Landauer approach hence does not apply if dissipation within the wire leads to thermalization.[24,25] The wire is assumed to be perfectly harmonic unless otherwise stated; reduction of thermal transport by anharmonic scattering is exponentially damped below the Debye temperature.[26]

The thermal conductance G of a nanowire with perfect transmission ($\mathcal{T}_i=1$) of harmonic vibrational modes from a thermal distribution at temperature T is $G=J/\delta T$, or

$$G = \frac{1}{2\pi\hbar} \int_0^\infty N(\omega) \frac{\hbar^3 \omega^2}{k_B T^2} \frac{e^{\hbar\omega/k_B T}}{(e^{\hbar\omega/k_B T} - 1)^2} d\omega. \quad (3)$$

Here $N(\omega)$ is the number of propagating modes at frequency ω and k_B is Boltzmann's constant. For a 3D elastic rod, such as a semiconductor nanowire, there are four modes that survive down to zero frequency: one torsional and one longitudinal mode, each with linear dispersion $\omega \sim k$, and two flexural models with quadratic dispersion $\omega \sim k^2$.

Note that this conductance is finite even if there is a perfect transmission of heat from one end of the wire to another: this is the thermal equivalent of the well known "contact resistance" in 1D electronic systems. If $N(\omega)$ is constant, so that $N(\omega)=N(\omega=0)$, we obtain in this ballistic limit

$$G = N(0) \frac{\pi^2 k_B^2 T}{3h}. \tag{4}$$

The same formula gives the leading behavior for small temperature T even if $N(\omega)$ is not constant, because in this limit the Bose-Einstein factor in the integral becomes concentrated near $\omega = 0$.

Elastic scattering is included in the Landauer approach through the "throughput" $\mathcal{T}(\omega) = \Sigma_i \mathcal{T}_i(\omega)$, which gives the fraction of incident energy flux on the left end that is transmitted through to the right end [hence $\mathcal{T}(\omega) = N(\omega)$, the number of modes, for clean systems with no scattering]. The conductance is then

$$G = \frac{1}{2\pi\hbar} \int_0^\infty \mathcal{T}(\omega) \frac{\hbar^3 \omega^2}{k_B T^2} \frac{e^{\hbar\omega/k_B T}}{(e^{\hbar\omega/k_B T} - 1)^2} d\omega. \tag{5}$$

The numbers $\mathcal{T}_i(\omega)$ for disordered 1D systems become exponentially small once the length of the 1D wire is larger than a "localization length" ξ that is determined by disorder strength and wire geometry. The analytic model of Maynard and Akkermans[15] on a pure 1D chain [$N(\omega) = 1$ for all allowed ω] with random masses can be summarized as follows: assume the throughput $\mathcal{T}(\omega)$ is unity for $L < \xi$ and zero for $L > \xi$, where the localization length ξ for the 1D linear chain follows from the results of Dyson[27] as follows:

$$\xi(\omega) = \frac{8\omega_D^2}{\sigma_M^2 \pi^2 \omega^2}. \tag{6}$$

Here σ_M^2 is the variance of the random mass distribution and ω_D is the Debye frequency. Note that the frequency dependence of ξ means that the same wire can be in the localized regime (i.e., $L \gg \xi$) for high frequencies, while in the ballistic regime (i.e., $L \ll \xi$) for low frequencies.

There are three regimes in a quasi-one-dimensional (multimode) wire. Let $\ell(\omega)$ be the mean free path averaged over the modes that propagate with frequency ω. At a given ω, if $N\ell \gg L$ then

$$\mathcal{T}(\omega) = \frac{N(\omega)}{1 + L/\ell(\omega)} + \mathcal{O}(N^0). \tag{7}$$

This equation describes ballistic behavior for $\ell(\omega) \gg L$, and for $N\ell \gg L \gg \ell$, Ohmic behavior in which the thermal conductance of a long wire decreases as the reciprocal of the length. If $N\ell \ll L$, then the phonons at frequency ω are effectively localized and

$$\mathcal{T} \sim e^{-L/\xi}, \tag{8}$$

where the localization length is $\xi = N\ell$. The number of propagating modes N clearly plays an important role in determining the crossover from Ohmic to localized transport.

These conclusions follow from noting that the same DMPK equation approach valid for electronic systems is appropriate for phonons, except that the dependence of the mean free path l on frequency is modified. The connection between $\mathcal{T}$ and the observed transport coefficient, expressed in the Landauer formula, is also different for electrons and phonons, since in the phonon case all frequencies with $\hbar\omega$ $\leq k_B T$ contribute significantly, while in the electronic case only frequencies within $k_B T$ of the Fermi level contribute significantly.

The DMPK equation is valid as long as phonon transfer matrices on scales longer than some mean free path become described by the orthogonal random matrix ensemble for one-dimensional systems.[23] While we cannot prove the validity of random-matrix theory assumptions for this problem, Sec. V verifies that the Ohmic (7) and localized (8) limits for $\mathcal{T}$ correctly describe thermal transport in a model system with *bulk* impurity scattering, while strongly localized transport in models with *boundary* scattering is not observed. Section IV explains how microscopic transmission coefficients are calculated via a transfer-matrix approach. In the next section we analyze the case of surface scattering.

III. STRONGLY DISORDERED SURFACE

It is typically assumed that the mean free path of a phonon due to surface scattering is on the order of d, the width of the material. In this section we show that this is not true for all phonon modes. Consider, for instance, the gapless modes (i.e., those that have vanishing wave vector perpendicular to the long direction of the rod). It is possible to estimate the mean free path of these modes using the following model. Consider a thin three-dimensional rod of length L, of square cross section with each edge of width d. Allow scalar waves to propagate on the strip, with Neumann boundary conditions. The dispersion relation is then

$$\omega = c\sqrt{k^2 + k_\perp^2}, \tag{9}$$

where $k_\perp = \sqrt{n_x^2 + n_y^2}(\pi/d)$, and $n_x, n_y = 0, 1, 2, \ldots$. We seek to calculate the mean free path due to surface scattering of the $n_x = 0$, $n_y = 0$ mode.

It can be shown using the methods of Ref. 19 that, for this mode, the mean free path is given by

$$\ell_0^{-1}(\omega) = 4(3\pi^2)^{2/3} \frac{h^2}{d^3} \left(\frac{\omega}{\omega_D}\right)^2 + 6\pi(3\pi^2)^{1/3} \frac{(h/a)^2}{d} \left(\frac{\omega}{\omega_D}\right)^4, \tag{10}$$

where h is the mean width of the disordered surface layer. c is the velocity of the gapless mode, and the correlation length scale for the surface disorder has been set to a, the lattice spacing. The first term comes from scattering back into the gapless mode, and the second into all other modes, and so involves a factor of the density of states, which scales like ω^2. The frequency dependence here is what one expects for scattering from pointlike impurities. The gapless mode, then, does not sense that the disorder is at the boundary: it sees the disorder as a collection of pointlike impurities. This frequency dependence ensures that at low temperatures the mode will be scattered weakly, and so will "reflect" almost specularly from the boundary.

This weak scattering of the gapless mode agrees with Rayleigh's criterion on the condition for specular reflection from a boundary. Rayleigh considered the following simplified model of a disordered surface: suppose the clean surface is a straight line at $y = 0$. Let the surface be at either $y = h/2$ or

$y=-h/2$. An incident wave then reflects from the disordered boundary as from two Bragg planes, a distance h apart. Define θ as the angle the incident wave makes with the surface. The phase difference between different parts of the reflected wave is then given by

$$\Delta\phi = 2\pi\frac{2h\sin\theta}{\lambda} = 2hk_\perp, \tag{11}$$

where $k_\perp$ is the component of the incoming wave vector perpendicular to the surface. If this phase difference $\Delta\phi$ is of order 1, then the reflected wave is destroyed through destructive interference, and the so wave must have been reflected diffusely. On the other hand, if $\Delta\phi \ll 1$, the reflection will be specular.

Consider now the phonon modes of the quasi-one-dimensional rod we considered above. One expects then that the modes with lower $k_\perp$ will scatter more weakly from the boundary than those with a larger value. As we increase $k_\perp$ through the value $1/h$, one expects a transition from modes with a long, frequency-dependent mean free path to modes with a mean free path of order d.

We can make an ansatz for the total throughput in the case of strong mode inequivalence, assuming that only the gapless mode has the frequency-dependent mean free path, and all others have a mean free path of d as follows:

$$\mathcal{T}(\omega) = \sum_i \frac{1}{1+L/\ell_i}, \tag{12}$$

where $\ell_i = \ell_0$ for the gapless mode and equals d for all other modes. This formula gives the DMPK form in the case of mode equivalence ($\ell_i = \ell$), and gives ballistic behavior if one of the mean free paths is much longer than the length of the system. We have assumed that the strongly scattered modes give an Ohmic contribution. In detail then, the throughput for the rod is

$$\mathcal{T}(\omega) = \frac{1}{1+L\ell_0^{-1}} + \frac{d}{L}\frac{(3\pi^2)^{2/3}}{8\pi}\frac{d^2}{a^2}\left(\frac{\omega}{\omega_D}\right)^2. \tag{13}$$

This is plotted for various widths in Fig. 2. This function can also be numerically integrated using Eq. (5) to find the corresponding thermal conductance as a function of frequency, $G(T)$. This is shown in Fig. 3.

The throughput is the sum of two contributions: the gapless mode gives a term that scales like $1/(1+C\omega^4)$, the other modes a term that scales like ω^2. Together, for a sufficiently thin rod, the dip in the throughput is somewhat smeared out by the exponential factors in the integral for $G(T)$, with the result that the thermal conductance is approximately linear in T up to about $T_D/5$.

It is also interesting to consider whether localization effects might be relevant. Let us assume that, at a frequency ω, there are of order $N(\omega)$ modes with a mean free path of d (we ignore for the moment the quasispecular modes). For this given mean free path, the localization length becomes $\xi(\omega) \simeq N(\omega)d$. For low frequencies, the number of modes is small, and so ξ should be of order the width of the system, which by assumption is much shorter than the length L.
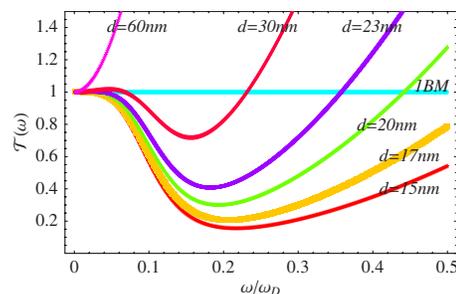

FIG. 2. (Color online) The throughput as a function of frequency for a surface-disordered rod, as suggested by Eq. (12). The length was chosen to be 2000 nm, a typical length for a nanowire. Here we have assumed that only the gapless mode has a frequency-dependent mean free path, and all others have a mean free path of order the width of the system, d. The label "1BM" stands for "one ballistic mode."

Hence all the low-frequency modes should be localized. As we increase the frequency, the number of modes increases like

$$N(\omega) \sim \left(\frac{\omega}{v/d}\right)^2 \sim \left(\frac{\omega}{\omega_D}\right)^2\left(\frac{d}{a}\right)^2 \tag{14}$$

and so at some value ω_* we will have $N(\omega_*)\alpha d = L$, or

$$\omega_* \sim \omega_D\sqrt{\frac{L/a}{(d/a)^3}} \sim 0.24\omega_D\left(\frac{22\text{ nm}}{d}\right)^{3/2}, \tag{15}$$

where we have set $a=0.543$ nm, the lattice constant of silicon, $L=2$ μm, a typical value for the length of a nanowire, and 22 nm was chosen as a comparison scale, since this is the width of the wire with anomalous thermal conductivity as observed by Li et al.[5] The frequency scale ω_* corresponds to a temperature scale of

$$T_* \sim 0.24T_D\left(\frac{22\text{ nm}}{d}\right)^{3/2}. \tag{16}$$

Under the assumption then these phonons have a mean free path due to boundary scattering of order d, one should ob-
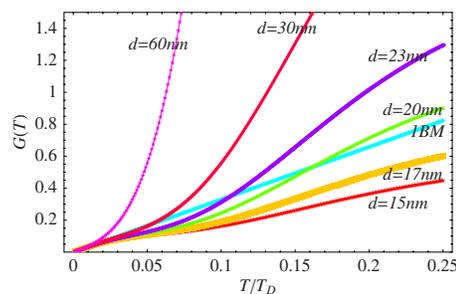

FIG. 3. (Color online) The thermal conductance associated with the throughput functions shown in Fig. 2. The scale for $G(T)$ is set by the curve for one ballistic mode (1BM). We have also included the correction due to umklapp scattering using the form suggested by Mingo (Ref. 8), but this correction is very small in the temperature range of interest.
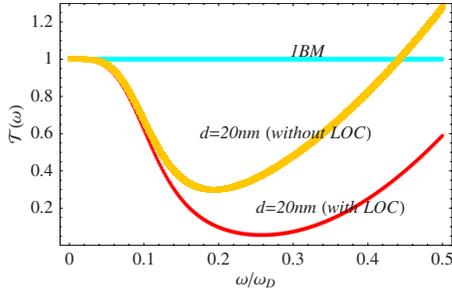
FIG. 4. (Color online) The throughput as a function of frequency for a surface-disordered rod, to illustrate the relevance of localization, based on the formula (17) in the text. As before, "1BM" stands for "one ballistic mode;" the "with loc" curve is based on the formula (17) in the text, and the "without loc" curve is identical to that of Fig. 2.

serve an exponentially small contribution to thermal transport at temperatures less than T_*.

These considerations are of course greatly complicated by the mixing with the quasispecular modes. The DMPK theory assumes that the transmitting channels are equivalent, and it is not known how the localization length changes when a quasiballistic mode is added to a number of strongly scattered modes. As an ansatz we approximate the quasiballistic mode as having decoupled from the strongly scattered modes. The resulting throughput is

$$\mathcal{T}(\omega) = \frac{1}{1 + L/\ell_0} + \frac{N(\omega)}{1 + L/d} e^{-L/(N(\omega)d)}. \quad (17)$$

The throughput and corresponding thermal conductances are shown in Figs. 4 and 5. Localization significantly reduces the thermal conductance below the incoherent limit.

A full understanding would require a theory that incorporates inequivalent channels, something that is not available at this time. Our numerical work described later sheds much light on this problem.

Note that in the high-frequency limit where it is possible to make a wave packet of phonons much smaller than the width of the wire, and this wave packet scatters like a particle, boundary scattering allows wave packets directed along the rod axis to pass through: this implies that true exponen-
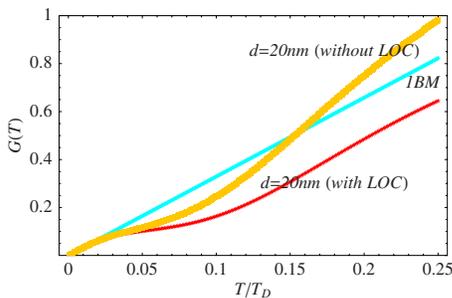

FIG. 5. (Color online) The thermal conductance associated with the throughput functions shown in Fig. 4. Again, the scale for $G(T)$ here is set by the one ballistic mode (1BM).

tial length dependence is not expected with boundary scattering, even when most thermal phonon modes are localized.

IV. DYNAMICAL TRANSFER-MATRIX APPROACH

First recall the definition of scattering and transfer matrices for waves. Let the amplitude in mode i that is incoming from the left be a_i, incoming from the right be d_i, outgoing to the left be b_i, and outgoing to the right be c_i. The index i ranges from 1 to $N(\omega)$.

The S matrix then maps the incoming amplitudes to the outgoing amplitudes

$$S \begin{pmatrix} \vdots \\ a_i \\ \vdots \\ d_i \\ \vdots \end{pmatrix} = \begin{pmatrix} \vdots \\ b_i \\ \vdots \\ c_i \\ \vdots \end{pmatrix}. \quad (18)$$

The matrix elements are given by

$$S = \begin{pmatrix} r & t' \\ t & r' \end{pmatrix}, \quad (19)$$

where r, t', t, and r' are all $N(\omega) \times N(\omega)$ matrices. The matrix elements have the following interpretation: r_{ij} is the amplitude for a left moving wave in mode i to be reflected to mode j, r'_{ij} is the amplitude for a right moving wave in mode i to be reflected into mode j, t_{ij} is the amplitude for a left moving wave in mode i to be transmitted into mode j, and t'_{ij} is the amplitude for a right moving wave in mode i to be transmitted into mode j.

For our purposes, the transfer matrix R will prove more useful. It is defined by

$$R \begin{pmatrix} \vdots \\ a_i \\ \vdots \\ b_i \\ \vdots \end{pmatrix} = \begin{pmatrix} \vdots \\ c_i \\ \vdots \\ d_i \\ \vdots \end{pmatrix}. \quad (20)$$

It has the property that if there are two regions in series labeled 0 and 1, then the total transfer matrix is given by $R = R_1 R_0$. It is not difficult to express R in terms of the transmission and reflection amplitudes as follows:

$$R = \begin{pmatrix} t - r't'^{-1}r & r't'^{-1} \\ -t'^{-1}r & t'^{-1} \end{pmatrix}. \quad (21)$$

The total transmission coefficient is obtained by taking the 22 element of R_1R_0, and inverting it: $t'_{0+1} = t'_0(1 - r_1r'_0)^{-1}t'_1$. This formula has a simple interpretation: write it as $t'_{0+1} = t'_0t'_1 + t'_0r_1r'_0t'_1 + t'_0r_1r'_0r_1r'_0t'_1 + \cdots$. It is evident that the total amplitude for transmission (from right to left) is given by the amplitude to get through the second obstacle and then the first obstacle; plus the amplitude to get through the second

obstacle, bounce off the first obstacle, bounce off the second obstacle, and then get through the first, ad infinitum.

Thermal transport by vibrational modes in a multimode wire requires a few modifications to the above equations: starting from coupled linear equations of motion for many ionic coordinates, we derive the form of the dynamical transfer matrix R that describes a longitudinal step along the wire. As an example, first consider a purely one-dimensional chain of balls connected by springs of constant strength C and mass m. Let u_i be the deviation, assumed small, of the position of ball i from its equilibrium location. The equation of motion for site i in the chain is

$$m\ddot{u}_i = C(u_{i+1} - u_i) + C(u_{i-1} - u_i). \tag{22}$$

The equation of motion at frequency ω can be written as follows:

$$\begin{pmatrix} u_{i+1} \\ u_i \end{pmatrix} = \begin{pmatrix} 2 - m\omega^2/C & -1 \\ 1 & 0 \end{pmatrix} \begin{pmatrix} u_i \\ u_{i-1} \end{pmatrix}. \tag{23}$$

Hence the matrix that corresponds to adding a single site in this coordinate basis is

$$M = \begin{pmatrix} 2 - m\omega^2/C & -1 \\ 1 & 0 \end{pmatrix}. \tag{24}$$

Now we convert this matrix to the basis of eigenmodes in order to obtain the transfer matrix R defined above.

An eigenmode of wave vector k_z satisfies (here a is the lattice spacing)

$$M \begin{pmatrix} u_i \\ u_{i-1} \end{pmatrix} = \lambda \begin{pmatrix} u_i \\ u_{i-1} \end{pmatrix}, \quad \lambda = e^{ik_z a}. \tag{25}$$

M is a real matrix and its eigenvalues form a time-reversed pair: they are either complex conjugates of each other (propagating modes in opposite directions) or reciprocal to each other (evanescent modes in opposite directions). The eigenvalues are

$$\lambda = 1 - \frac{m\omega^2}{2C} \pm \frac{m\omega\sqrt{\omega^2 - 4C/m}}{2C} \tag{26}$$

describing propagating modes with k_z real if $m\omega^2 < 4C$ and evanescent modes with k_z imaginary if $m\omega^2 > 4C$. Consider the regime of propagating modes: in this basis the transfer matrix becomes just

$$R = \begin{pmatrix} \lambda & 0 \\ 0 & \lambda^* \end{pmatrix}, \tag{27}$$

which gives a unitary S matrix since

$$S = \begin{pmatrix} 0 & \lambda \\ \lambda^* & 0 \end{pmatrix} \tag{28}$$

and $|\lambda| = 1$.

The same procedure applies in a multimode wire except that now r, t, r', and t' are matrices. There is one technical difference that appears between the vibrational case and the standard electronic case. In the vibrational case, it is the energy flux rather than the probability flux that satisfies a continuity equation. Hence the basis in which the S matrix is (almost) unitary is one in which incoming and outgoing excitations are normalized to unit energy flux, rather than unit probability flux. Actually the whole S matrix is not unitary, but only the portion made up of modes with nonzero energy flux.[28]

Note that the transfer-matrix approach used in this paper to make contact with mesoscopic electron physics works at a fixed frequency ω (equivalent to fixed energy in the electronic case). The extension of the above to an extended 1D wire with random masses or spring constants is as follows: First, the eigenmodes in the absence of disorder are obtained from the transfer matrix above. Then the transmission coefficients for these modes through a disordered system are obtained by combining many individual segments (with different transfer matrices). After the transmission coefficients for a fixed disorder realization are obtained as a function of ω, a final integration step gives the thermal conductance for that realization as a function of temperature. (Note that the first step of this approach, obtaining the eigenmode spectrum without disorder, is different computationally from typical dynamical matrix calculations in which k_z is fixed and the frequencies ω of different phonon bands are obtained but obtains the same spectrum of propagating modes.)

In the multimode case, the transfer matrix R describes how incident and outgoing modes at the left edge of a region are matched to incident and outgoing modes at the right edge of the region. Once there is disorder in the system, energy flux incident in mode i will be distributed over reflected modes, other transmitted modes, and the original mode, with conservation of energy flux. The Landauer expression for the thermal conductance in Sec. II contains a sum over $\mathcal{T}_i$; $\mathcal{T}_i$ is defined as the fraction of the incident energy flux in mode i that reaches the other end of the sample, i.e., $\mathcal{T}_i = \Sigma_j |t_{ij}|^2$. In the next section we show numerical results on the thermal conductance of two-dimensional disordered strips.

V. THERMAL CONDUCTANCE OF QUASI-ONE-DIMENSIONAL SYSTEMS: NUMERICAL RESULTS

A. Two-dimensional strip

This section applies the transfer-matrix approach outlined in the previous section to a simple harmonic "ball-and-spring" model system with ions moving in two dimensions. Considerable previous work[29] has shown in the absence of disorder that similar models, possibly including next-neighbor and bond-angle terms, can describe the phonon spectra of quasi-one-dimensional systems (including carbon nanotubes) with ions moving in three dimensions. The justification for studying a model system with only two-dimensional motion is that already in two dimensions both linearly and quadratically dispersing modes are present, as in 3D, and the analytic predictions in Sec. II can be checked comprehensively by going to very large wire sizes. The following section (Sec. V B) sets out experimental predictions for semiconductor nanowires in 3D based on the analytic picture outlined in Sec. II and checked below.

The existence of gapless modes in a vibrational system is related to the Euclidean motions of a rigid body: the gapless
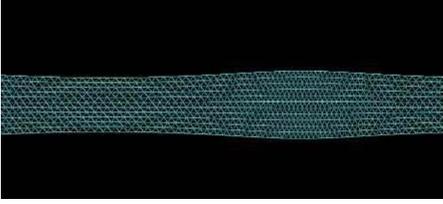
FIG. 6. (Color online) The acoustic longitudinal mode of a strip of triangular lattice.

vibrational modes are those that become symmetries, typically translations, in the long-wavelength limit. There are four gapless modes in a rod, rather than three as in a bulk solid, because rotation around the rod axis guarantees a gapless "torsional" mode in addition to flexural and compressional modes that become translations along the three axes. For a rigid wire moving in two dimensions, there are two gapless modes: using $\hat{z}$ to denote the rod axis, there is a linearly dispersing longitudinal mode with displacements along $\hat{z}$ in the long-wavelength limit, and a quadratically dispersing flexural mode with displacements along $\hat{x}$. Additional modes begin to propagate as the frequency is increased.

The simplest rigid body in two dimensions is the triangular lattice with springs connecting lattice points. (The square lattice has vanishing rigidity in 2D if the potentials are purely length-dependent nearest-neighbor springs.) The longitudinal mode for this system is shown in Fig. 6 and the flexural mode is shown in Fig. 7.

A simple model for the number of propagating modes agrees qualitatively with the numerical results for this quantity. The system has two modes as $\omega \to 0$—the longitudinal and flexural acoustic modes. As we increase ω to $\sim \pi v/2d$, where d is the width, we expect to encounter modes that have a finite wavelength in the transverse direction. If we assume, in a simplified picture, that at each $\omega = n\pi v/2d$ we add two more modes to $N(\omega)$, and that every mode has the same velocity, then the number of modes is approximately given by

$$N(\omega) = 2 + \frac{4d}{\pi v}\omega. \tag{29}$$

For $\omega > \omega_D$, where ω_D is the Debye frequency, the lowest-lying modes are no longer propagating, and so one expects the number of modes to decrease, with approximately the same slope.
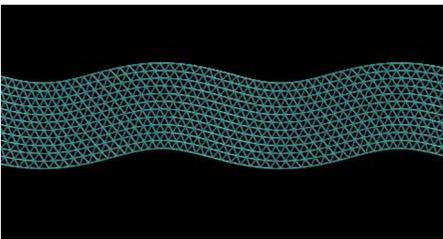

FIG. 7. (Color online) The acoustic flexural mode of a strip of triangular lattice.

In what follows we will assume that $N(\omega)$ has the form

$$N(\omega) = 2 + c\frac{d\omega}{\omega_D}, \tag{30}$$

where c is a constant of order unity, and d, the width, is now measured in units of the lattice spacing.

1. Bulk disordered

Consider the case where the isotopic disorder extends throughout the material (in a later section we will constrain the disorder to be at the edge of the strip). The rate at which waves scatter from pointlike defects is determined by the Rayleigh-Klemens formula as follows:[30]

$$\tau(\omega)^{-1} = \sigma^2\omega^2\left(\mathcal{D}\frac{\omega^{\mathcal{D}-1}}{\omega_D^{\mathcal{D}}}\right), \tag{31}$$

where $\mathcal{D}$ refers here to the dimension of the space, and σ^2 is the fluctuation in a single mass. The DMPK formalism suggests a formula for the total throughput of a quasi-one-dimensional system in the ballistic and Ohmic regimes as follows:

$$\mathcal{T}(\omega) = \frac{N(\omega)}{1 + L/\ell(\omega)}. \tag{32}$$

As the length of the system L extends belong the mean free path ℓ, the throughput (and hence the contribution of that frequency to the thermal conductance) scales like $1/L$; this is a feature characteristic of Ohmic systems.

From the Rayleigh-Klemens formula, one anticipates a mean free path of

$$\frac{1}{\ell(\omega)} \sim \frac{1}{v}\sigma^2\omega^2 N(\omega). \tag{33}$$

In the Ohmic limit this suggests a length and frequency scaling in the throughput of

$$\mathcal{T}(\omega) \simeq \frac{N(\omega)\ell(\omega)}{L} \sim \frac{N(\omega)}{L}\frac{1}{\omega^2 N(\omega)} \sim \frac{1}{L\omega^2}. \tag{34}$$

As an example of the throughput of a bulk-disordered system, see Fig. 8. The strip chosen was of width 32 sites, and of varying lengths as shown in the legend. In each case, the probability that a given site was replaced by an disordered site is $1/32$. Here the disordered sites were chosen to have mass $1+\sqrt{2}$, whereas the original masses are 1. Note that this can be used to model any substitutional disorder, since the effects of a change in spring constants or a strain field can be absorbed into σ^2 (see Ref. 30).

The general shape of the curves in Fig. 8 is consistent with the DMPK formula for the throughput, with the frequency-dependent mean free path given by the Rayleigh-Klemens formula. For small frequencies, the phonon scattering rate is small, and so the total throughput tracks the number of modes. As the frequency increases, the phonons are more strongly scattered; the mean free path decreases faster than the density of states increases, and so the throughput decreases with increasing frequency.
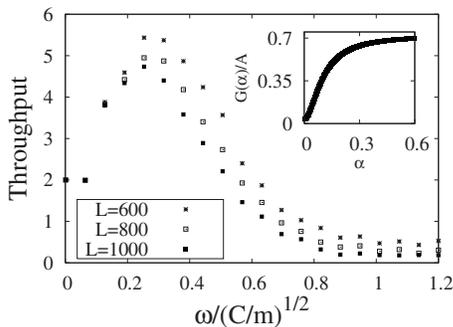
FIG. 8. The throughput as a function of frequency for a two-dimensional strip of width 32 sites. The various lengths are shown in the legend. The throughput shown has been averaged over 40 implementations of the disorder, as described in the text. The inset shows the thermal conductance corresponding to the throughput for $L=1000$ shown in the main figure. This was found by numerical integration using Eq. (5). The quantity α is a dimensionless temperature defined by $\alpha=(k_BT)/(\hbar\sqrt{C/m})$, where C is the spring constant; A is a constant defined as $A=(k_B/2\pi)\sqrt{C/m}$.

The thermal conductance as a function of temperature corresponding to the $L=1000$ throughput is shown in the inset of Fig. 8.

The dependence of the throughput on L and ω is considered in Fig. 9. In the inset the throughput multiplied by the length is plotted as a function of frequency. The throughput clearly scales like $1/L$ in the frequency regime shown. The line shown in the figure demonstrates the scaling with frequency, which is of the form $\sim\omega^{-2.6}$.

The throughput for the localized regime is illustrated in the main figure of Fig. 9. As the Ohmic throughput $\mathcal{T}\sim N\ell/L$ decreases to a value less than 1, the throughput decreases faster than any power law.

2. Edge disordered

We consider in this section the throughput of the two-dimensional strip with only the boundary of the strip disor-
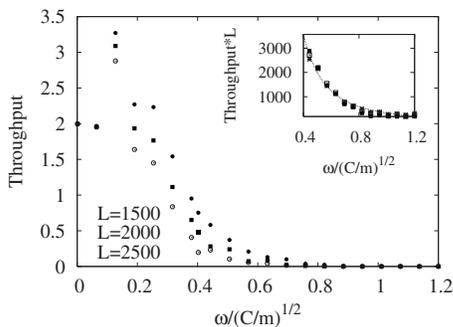

FIG. 9. The throughput as a function of frequency for a bulk-disordered strip of width 32 sites and various lengths. The alloy fraction here is 0.1. As the throughput passes through 1, it tends to zero faster than any power. The inset shows the same data as Fig. 8; here though the throughput has been multiplied by the length of the system, to make the $1/L$ dependence more clear. The curve shown is given by a constant multiplied by $\omega^{-2.6}$.
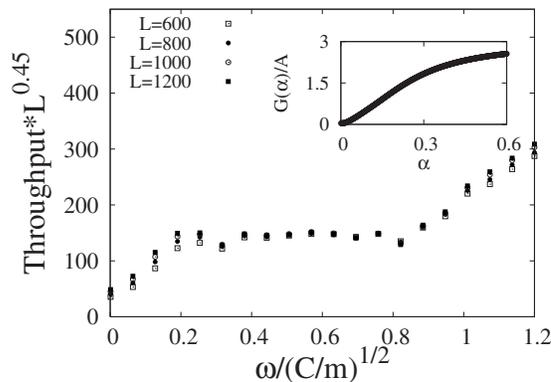

FIG. 10. Throughput of a strip of width 48 sites multiplied by $L^{0.45}$ as a function of frequency for the case where the disordered is only at the edge. The reason for the kink at higher frequency is unclear. The inset shows the thermal conductance corresponding to the $L=1000$ throughput. The quantities α and A are defined as in Fig. 8: $\alpha=(k_BT)/(\hbar\sqrt{C/m})$, and $A=(k_B/2\pi)\sqrt{C/m}$.

dered. Recall that in the case of bulk disorder, the throughput shows a strong frequency dependence—essentially because the mean free path is set by Rayleigh-Klemens formula for scattering from pointlike defects. In contrast, when the disorder is present only at the edge, a more appropriate model is that the phonons are scattered, specularly or diffusively, at the boundary.

The throughput is shown as a function of frequency for various lengths in Fig. 10. The throughput was calculated by disordering a region of thickness 1 site at both edges of the strip. The mass of these edge sites was chosen at random to be either 1 (the mass in the clean case) or $1+\sqrt{2}$, each with probability $1/2$. The throughput was then calculated numerically as described earlier. The figure shows the throughput averaged over 40 implementations of the disorder.

From the figure one can see that once the phonon frequency is no longer in the ballistic regime, the throughput levels off to approximately a constant. A throughput that is constant as a function of frequency can be seen experimentally as a thermal conductance that is linear in temperature: if the throughput is equal to, say, c, then the thermal conductance is cg_0, where g_0 is the quantum of thermal conductance. Again the inset shows the thermal conductance as a function of temperature for the $L=1000$ throughput. The throughput has been rescaled to remove the length dependence. Note that the throughput scales like $1/L^\beta$, where β is less than 1: the system is not in the Ohmic regime.

To illustrate the reason for the frequency-independent throughput, we show the mode-resolved throughput in Fig. 11. Here, for each mode, a unit flux was incident on the disordered region. The total flux that is transmitted into any mode (corresponding, for the ith mode, to $\mathcal{T}_i$) was recorded. For the bulk-disordered case, all modes are equivalent. However, for the edge-disordered case, the throughput is dominated by two modes in the frequency range in which it is constant. These modes happen to have a small displacement at the boundary. Their contribution is approximately constant.

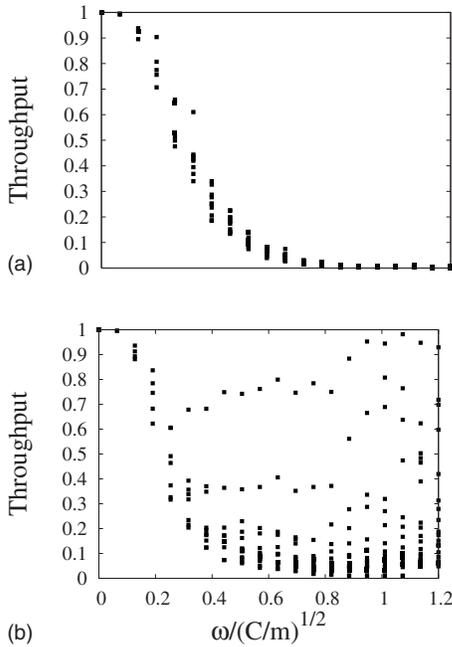When the disorder is exclusively at the boundary, the boundary displacement of the different modes will obviously

FIG. 11. Mode-resolved throughput of a strip of width 32 sites as a function of frequency for the case where the disordered is distributed throughout the bulk (top), or at the edge (bottom) of the material. The length of the strip in both cases is 1600 sites.

determine how strongly they are scattered—a mode with vanishing boundary displacement will pass through the material ballistically.

In addition, these boundary displacements can vary dramatically for different modes at the same frequency. For instance, when ω is such that $\omega > v/d$, the ungapped longitudinal and flexural modes become surface waves. This occurs because a surface wave must decay exponentially into the bulk. Its dispersion must then be $\omega \sim v\sqrt{k_z^2 - k_x^2}$. Therefore for a given ω, these surface modes have the largest k_z among all the propagating modes: this identifies them as a linear combination of the flexural and longitudinal modes.

By contrast, the first set of gapped modes tend to have an anomalously small displacement at the boundary. This is illustrated in Table I. For a frequency of $\omega = 0.57\sqrt{C/m}$ (C is the spring constant), and a width of 32 sites, the k_z values of the various propagating modes along with the amount of displacement at the boundary is shown. By boundary displacement we mean the displacement summed over the two sites at the edge of the strip. The modes here are normalized to 1/2: a mode with boundary displacement squared 1/2 would exist exclusively at the top and bottom sites of the strip.

B. Three-dimensional rod

In this section we consider numerical data for a three-dimensional rod. The system we study has 127 atoms in a cross section, as shown in the inset of Fig. 12. The atoms are arranged in a triangular lattice, with springs connecting nearest neighbors and next-to-nearest neighbors. At small frequencies there are four normal modes: longitudinal, tor-

TABLE I. Boundary displacements $|\vec{\phi}|^2$ for the 14 propagating modes at frequency $\omega = 0.57\sqrt{C/m}$ for a strip of width 32 sites. The wave vectors are measured in units of the inverse lattice spacing. The units of $|\vec{\phi}|^2$ are arbitrary: we wish to point out only that some modes have almost vanishing boundary displacement.

k_{zj}	$|\vec{\phi}|^2$
1.059383	0.189611
1.059383	0.189612
0.929791	0.002395
0.904105	0.008771
0.854861	0.016750
0.773922	0.024001
0.657264	0.033273
0.558262	0.088231
0.526373	0.087008
0.525994	0.025183
0.447062	0.076678
0.442868	0.038433
0.275598	0.062901
0.293598	0.045720

sional, and two flexural. The longitudinal and torsional modes disperse linearly, while the flexural disperse quadratically.

The rods are disordered in the same way as described for the strip. In the clean case each atom has mass 1; for a disordered system each atom is replaced by an atom of mass $1 + \sqrt{2}$ with a certain probability, the alloy fraction. As before, we will consider both bulk (i.e., each atom in a given cross section can be replaced) and boundary (i.e., only those atoms at the outer edge of the cross section can be replaced) disorder.

We find the throughput using the transfer-matrix method. In Fig. 12, we show the disorder-averaged throughput for a rod of length 100 sites. Both bulk- and boundary-disordered
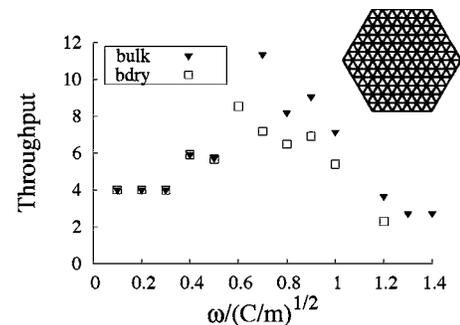

FIG. 12. Disorder-averaged throughput for a rod of length 100 sites as a function of frequency. Both the bulk- and boundary-disordered cases are shown. On the top right a cross section of the nanowires considered is shown. There are, in fact, springs connecting next-to-nearest neighbors (spring constant 0.4) as well as nearest neighbors (spring constant 1.0), although they are not shown here.

cases are shown. The alloy fraction for the bulk case was chosen to be 0.1; for the boundary case it was chosen to be 12.7/36: this ensures that the number of disordered atoms in a cross section is the same for the bulk- and boundary-disordered cases.

The data show that the throughput in the case of boundary scattered rods is noticeably less than the bulk-disordered case. This is because phonon modes in a rod tend to have more displacement at the edge than at the center, since at the edge the masses have greater freedom to vibrate.[31]

One feature which is not apparent is the presence of modes which have a displacement at the boundary orders of magnitude smaller than that of the other modes (recall that these modes dominated the throughput of the edge-disordered strip). This may be due to the relatively small diameter of the rod considered here: in the data shown, we have not, in fact, reached the limit where the surface waves have formed.

Finally, it is interesting to note that the reflection and transmission matrices for a short system can be used to find the incoherent limiting conductance. If the transmission and reflection matrices for a system of length δL are $\widetilde{T}$ and $\widetilde{R}$, then the transmission and reflection matrices for a system of length $n\delta L$ (denoted T_n and R_n) are

$$T_n = \widetilde{T}(1 - R_{n-1}\widetilde{R})^{-1}T_{n-1}, \tag{35}$$

$$R_n = R_{n-1} + T_{n-1}\widetilde{R}(1 - R_{n-1}\widetilde{R})^{-1}T_{n-1}. \tag{36}$$

This may prove useful to isolating the incoherent signal in future studies.

VI. CONCLUSION

In conclusion, we have studied the thermal conductance of insulating nanowires at low temperatures. For the thinnest wires, with diameters of order 20 nm, it was argued that frequency-dependent surface scattering is relevant. In particular, modes with a small $k_\perp$ (i.e., the component of the wave vector in the direction perpendicular to the long direction of the wire) should scatter almost specularly from the boundary, whereas those with a larger $k_\perp$ presumably have a mean free path of order d, the width of the wire. The resulting thermal conductance is shown in Fig. 3, for a number of diameters. For a width $d=20$ nm, the thermal conductance is almost equal to that of a single ballistic mode. This can be understood as follows. There are two contributions to the thermal conductance: that of the quasispecular modes, whose number is fixed but whose contribution decreases with increasing frequency; and the diffusively scattered modes, whose mean free path is fixed but whose number increases with frequency. These decreasing and increasing terms together give an approximately constant throughput for low frequencies (Fig. 2).

These considerations also suggest strongly that localization effects are relevant to transport in nanorods of transverse dimension $d \lesssim 20$ nm. This was demonstrated by applying the DMPK formalism, which at certain frequencies is not valid—DMPK requires mode equivalence, and at small frequencies the quasispecular mode has a mean free path much longer than the other modes. Nevertheless, it would be of great interest to explore experimentally localization phenomena in these nanowires. For instance, a different temperature dependence in the thermal conductance and heat capacity, with the heat capacity measured through a bulk contact to a reservoir, would be strong evidence that some of the phonon modes are localized.

In order to understand the relevance of coherence effects, we have also simulated phonon transport using a dynamical transfer-matrix method. Our simulations show a mode inequivalence for the case of scattering from a disordered surface that is not present when the impurities are placed at random throughout the strip. The total throughput of the surface-disordered strip is approximately constant in frequency, consistent with a linear thermal conductance.

If the ballistic and strongly scattered modes were decoupled, one would expect some modes to have a throughput of approximately 1, and others to have an exponentially small throughput. Although the mode inequivalence we observe numerically is not that strong, the total throughput is consistent with the picture that some modes are quasiballistic, and the rest are strongly scattered. Also, the throughput for the surface scattering case shows a non-Ohmic behavior approximately described by a power law: $\mathcal{T}(\omega) \sim 1/L^\beta$ with $\beta < 1$. This is consistent with the presence of quasiballistic modes.

An additional effect brought to light by our simulations is the highly variable displacement that phonon modes can have at the boundary of the nanowire. We found that whereas the gapless modes acquire a large boundary displacement, other modes acquire anomalously low values. These were the modes that gave a quasiballistic contribution to transport. Our dynamical transfer-matrix method could be applied to specific crystal structures and materials of interest by using parameters from full *ab initio* simulations of nanowires, including boundary effects.

Note added in proof. In a forthcoming paper, Ref. 32, we use a slightly simplified form of the theory presented here to fit thermal conductance data for silicon nanowires.

ACKNOWLEDGMENTS

[1] K. Schwab, E. A. Henriksen, J. M. Worlock, and M. L. Roukes, Nature (London) **404**, 974 (2000).

[2] L. G. C. Rego and G. Kirczenow, Phys. Rev. Lett. **81**, 232 (1998).

[3] D. H. Santamore and M. C. Cross, Phys. Rev. Lett. **87**, 115502 (2001).

[4] Y. Tanaka, F. Yoshida, and S. Tamura, Phys. Rev. B **71**, 205308 (2005).

[5] D. Y. Li, Y. Y. Wu, P. Kim, P. D. Yang, and A. Majumdar, Appl. Phys. Lett. **83**, 2934 (2003).

[6] D. Y. Li, Y. Wu, R. Fan, P. D. Yang, and A. Majumdar, Appl. Phys. Lett. **83**, 3186 (2003).

[7] P. Kim, L. Shi, A. Majumdar, and P. L. McEuen, Phys. Rev. Lett. **87**, 215502 (2001).

[8] N. Mingo, Phys. Rev. B **68**, 113308 (2003).

[9] L. S. Froufe-Pérez, P. García-Mochales, P. A. Serena, P. A. Mello, and J. J. Sáenz, Phys. Rev. Lett. **89**, 246403 (2002).

[10] M. P. Blencowe, J. Phys.: Condens. Matter **7**, 5177 (1995).

[11] A. Kambili, G. Fagas, V. I. Fal'ko, and C. J. Lambert, Phys. Rev. B **60**, 15593 (1999).

[12] B. J. van Wees, H. van Houten, C. W. J. Beenakker, J. G. Williamson, L. P. Kouwenhoven, D. van der Marel, and C. T. Foxon, Phys. Rev. Lett. **60**, 848 (1988).

[13] L. G. C. Rego and G. Kirczenow, Phys. Rev. B **59**, 13080 (1999).

[14] M. P. Blencowe and V. Vitelli, Phys. Rev. A **62**, 052104 (2000).

[15] R. Maynard and E. Akkermans, Phys. Rev. B **32**, 5440 (1985).

[16] D. E. Angelescu, M. C. Cross, and M. L. Roukes, Superlattices Microstruct. **23**, 673 (1998).

[17] M. P. Blencowe, Phys. Rev. B **59**, 4992 (1999).

[18] G. Fagas, A. G. Kozorezov, C. J. Lambert, J. K. Wigmore, A. Peacock, A. Poelaert, and R. den Hartog, Phys. Rev. B **60**, 6459 (1999).

[19] D. H. Santamore and M. C. Cross, Phys. Rev. B **63**, 184306 (2001).

[20] P. B. Allen, J. L. Feldman, J. Fabian, and F. Wooten, Philos. Mag. B **79**, 1715 (1999).

[21] O. N. Dorokhov, JETP Lett. **36**, 318 (1982).

[22] P. A. Mello, P. Pereyra, and N. Kumar, Ann. Phys. (N.Y.) **181**, 290 (1988).

[23] C. W. J. Beenakker, Rev. Mod. Phys. **69**, 731 (1997).

[24] S. Nose, J. Chem. Phys. **81**, 511 (1984).

[25] W. G. Hoover, Phys. Rev. A **31**, 1695 (1985).

[26] N. W. Ashcroft and N. D. Mermin, *Solid State Physics* (Holt, Rinehart and Winston, New York, 1976).

[27] C. Itzykson and J.-M. Drouffe, *Statistical Field Theory* (Cambridge University Press, Cambridge, 1991), Vol. 2.

[28] If λ_i are the amplitudes in orthogonal incident modes i with energy flux v_i, while λ_o are the amplitudes of orthogonal outgoing modes o with flux v_o, then the flux conservation condition is

$$\sum_i |\lambda_i|^2 v_i = |\lambda_o|^2 v_o,$$

which becomes equivalent to a unitarity condition if all modes have nonzero flux. In general, evanescent modes are required to make a complete eigenbasis but have zero energy flux; in this case the requirement of flux conservation does not affect elements of the S matrix that involve evanescent modes. For example, for $m\omega^2 > 4$ in the above example the S matrix is non-unitary in the eigenmode basis but energy flux is still conserved.

[29] G. D. Mahan and G. S. Jeon, Phys. Rev. B **70**, 075405 (2004).

[30] P. G. Klemens, Proc. Phys. Soc., London, Sect. A **68**, 1113 (1955).

[31] K. Graff, *Wave Motion in Elastic Solids* (Dover, New York, 1991).

[32] R. Chen *et al.* (unpublished).